

Energy optimization of a wastewater treatment plant based on energy audit data: small investment with high return

*Original*

Energy optimization of a wastewater treatment plant based on energy audit data: small investment with high return / Borzooei, S.; Amerlinck, Y.; Panepinto, D.; Abolfathi, S.; Nopens, I.; Scibilia, G.; Meucci, L.; Zanetti, M. C.. - In: ENVIRONMENTAL SCIENCE AND POLLUTION RESEARCH INTERNATIONAL. - ISSN 0944-1344. - 27:15(2020), pp. 17972-17985. [10.1007/s11356-020-08277-3]

*Availability:*

This version is available at: 11583/2840594 since: 2020-07-17T15:13:25Z

*Publisher:*

Springer

*Published*

DOI:10.1007/s11356-020-08277-3

*Terms of use:*

This article is made available under terms and conditions as specified in the corresponding bibliographic description in the repository

*Publisher copyright*

(Article begins on next page)

1           **Energy Optimization of a Wastewater Treatment Plant based on Energy**  
2           **Audit Data: Small Investment with High Return**

3  
4  
5 Sina Borzooei<sup>1\*</sup>, Youri Amerlinck<sup>2</sup>, Deborah Panepinto<sup>1</sup>, Soroush Abolfathi<sup>3</sup>, Ingmar Nopens<sup>2</sup>  
6 Gerardo Scibilia<sup>4</sup>, Lorenza Meucci<sup>4</sup>, Maria Chiara Zanetti<sup>1</sup>  
7  
8

9 1. Department of Environment, land and infrastructure Engineering (DIATI), Politecnico di  
10 Torino, Torino, Italy.  
11

12 2. BIOMATH, Department of Data Analysis and Mathematical Modelling, Faculty of Bioscience  
13 Engineering, Ghent University, Coupure Links 653, 9000 Gent, Belgium  
14

15 3. Warwick Water Research Group, School of Engineering, The University of Warwick, Coventry  
16 CV4 7AL, UK  
17

18 4. SMAT (Società Metropolitana Acque Torino) research center, Corso Unità d'Italia 235/3,  
19 10127, Torino (TO), Italy  
20

21  
22 \*Corresponding author: sina.borzooei@polito.it  
23

24 This is the pre-print version of manuscript. The post-print version can be found online:

25 <https://doi.org/10.1007/s11356-020-08277-3>

26 The request can be sent to authors to receive the complete version of the manuscript.  
27  
28  
29  
30  
31  
32  
33  
34  
35  
36  
37

1 **Abstract:**

2 Ambitious energy targets in the 2020 European climate and energy package have encouraged many  
3 stakeholders to explore and implement measures improving the energy efficiency of water and  
4 wastewater treatment facilities. Model-based process optimization can improve the energy  
5 efficiency of wastewater treatment plants (WWTP) with modest investment and a short payback  
6 period. However, such methods are not widely practiced due to the labor-intensive workload  
7 required for monitoring and data collection processes. This study offers a multi-step simulation-  
8 based methodology to evaluate and optimize the energy consumption of the largest Italian WWTP  
9 using limited, preliminary energy audit data. An integrated modeling platform linking wastewater  
10 treatment processes, energy demand, and production sub-models is developed. The model is  
11 calibrated using a stepwise procedure based on available data. Further, a scenario-based  
12 optimization approach is proposed to obtain the non-dominated and optimized performance of the  
13 WWTP. The results confirmed that up to 5000 MWh annual energy saving in addition to improved  
14 effluent quality could be achieved in the studied case through operational changes only.

15 **Keywords:** Wastewater treatment plant; Energy efficiency; Data scarcity; Energy audit; Activated  
16 sludge model; Energy optimization; Calibration; Process optimization

17

18

19

20

21

22

23

24

25

26

27

## 1 Nomenclature

---

ASM	Activated sludge model
$b_A$	Autotrophic decay rate
BME	Combined Blower and Motor Efficiency
BNRAS	Biological Nutrient Removal activated sludge
BOD <sub>5</sub>	5-day biochemical oxygen demand
BSM1	Benchmark Simulation Model No 1
$C_c$	Clarification coefficient
COD	Chemical oxygen demand
COD <sub>s</sub>	Soluble chemical oxygen demand
COD <sub>t</sub>	Total chemical oxygen demand
$C_p$	Heat capacity of air at constant pressure
CSTR	Completely Stirred Tank Reactor
$d_a$	Airflow per diffuser
$d_d$	Diffuser submergence depth
$d_{de}$	Diffuser density
DO	Dissolved Oxygen concentration
$e$	Combined blower and motor efficiency
$E_{Ca}$	Aeration energy consumption
$E_{Cm}$	Mixing energy consumption
$E_{Cp}$	Pumping energy consumption
$E_{Ct}$	Total energy consumption
$E_{Pw}$	Total energy produced from WAS
EQI	Effluent Quality Index
$F_c$	Correction factor
$F_f$	Fouling factor
GHG	Greenhouse gas
HC-D	High-load condition in dry-weather operational mode
HC-W	High-load condition in wet-weather operational mode
$H_d$	Dynamic head
HRT	Hydraulic retention time
$H_s$	Pumping head
$H_{st}$	Static head
$I_c$	Current absorption
IMLR	Internal Mixed Liquor Recycle
$K$	Dynamic head-loss coefficient
$K_c$	Proportional gain
$K_{OA}$	Oxygen half-saturation index for autotrophic biomass
MLE	Modified Ludzack-Ettinger
MLSS	Mixed Liquor Suspended Solids
NC-D	Normal condition in dry-weather operational mode
OTE	Oxygen Transfer Efficiency
PAC	Performance Assessment criterion
$P_D$	Delivered power blower
$P_e$	Pump efficiency
$P_{FL}$	Pipe friction loss
PI	Proportional Integral
$P_{PUV}$	Power Per Unit Volume of mixing
PS	Primary Sludge
$P_s$	Barometric pressure

$Q$	Pumping flow rate
$Q_{IMLR}$	Internal Mixed Liquor Recirculation flowrate
$Q_N$	Normalized air flux
$Q_{RAS}$	Return activated sludge flowrate
$R$	Universal gas constant
RAS	Return Activated Sludge
RWS	Reject Water from Sludge treatment units
SCADA	Supervisory Control and Data Acquisition
SOTE	Standard Oxygen Transfer Efficiency
SRT	Solids Retention Time
STOWA	Acronym for the foundation for applied water research in Netherlands
SVI	Sludge volume Index
$T_a$	Blower inlet air temperature
$T_i$	Integral time
TKN	Total Kjeldahl Nitrogen
TN	Total Nitrogen
TP	Total phosphorous
TSS	Total Suspended Solid
VS	Volatile Solids
VSS	Volatile Suspended Solids
$w$	Mass of the airflow
WAS	Wasted Activated Sludge
WWTP	Wastewater Treatment Plant
$\alpha$	The ratio of process water to clean water mass transfer coefficients
$\Delta P_d$	The pressure drop of the piping and diffuser downstream of the blower
$\mu_A$	The maximum specific growth rate for autotrophic biomass
$\phi$	Power factor

---

1

2

3

4

5

6

7

8

9

## 1 **1. Introduction**

2 The emerging trend of water scarcity resulted from population growth, and climate change has  
3 increased pressure on water and wastewater industries. Urban water systems require a considerable  
4 amount of energy for water transportation and treatment. Hence, high energy demand can  
5 potentially become an impediment to sustainable urban areas and cause water pollution, as well as  
6 a shortage of water resources. Water and wastewater treatment plants (WWTP) are amongst the  
7 largest municipal energy consumers and thus one of the most significant contributors to  
8 greenhouse gas (GHG) emissions (Guerrini et al., 2017). To exemplify, 22,558 WWTPs are  
9 operating throughout the European Union (EU), consuming almost 15,021 GWh/year, which is  
10 more than 1% of the overall electricity consumption in the EU (Eurostat, 2013). Country-specific  
11 studies about Germany (Reinders et al., 2012) and Italy (Foladori et al., 2015) showed that  
12 electricity demand for WWTPs only accounts for almost 1% of total energy consumption in these  
13 countries. A study (US EPA, 2012) about drinking and wastewater treatment systems in the United  
14 States, proved that they account for 3 - 4% of overall energy use, which results in more than 45  
15 million tons of annual GHG emissions. From an economic point of view, energy consumption of  
16 a conventional WWTP constitutes about 25 - 40 % of entire operating costs, corresponding to the  
17 range of 0.3 – 2.1 kWh/m<sup>3</sup> of treated wastewater (Elías-Maxil et al., 2014; Venkatesh and Brattebø,  
18 2011).

19 The major GHGs emanating from WWTPs are carbon dioxide (CO<sub>2</sub>), methane (CH<sub>4</sub>), and nitrous  
20 oxide (N<sub>2</sub>O), which are mainly produced in microbial activities, nitrification, and denitrification  
21 stages and anaerobic digestions, respectively (Nguyen et al., 2019). Several studies focused on  
22 direct measurement and monitoring of GHGs in WWTPs (e.g., Amerlinck et al., 2016; Bellandi et  
23 al., 2018; Caivano et al., 2017; Kiselev et al., 2019), highlighting the wastewater treatment sector  
24 as an area of concern for the today's global warming issue.

25 Overall, due to the increasing cost of energy and growing worldwide concerns about GHG  
26 emissions and climate change, the issue of energy efficiency in WWTPs has gained significant  
27 attention (Friedrich et al., 2009).

28 Process optimization of WWTPs can significantly increase energy efficiency with meager  
29 investment and a short payback period (Descoins et al., 2012). Full-scale evaluation of any  
30 optimization strategy is an expensive and time-consuming task, which may increase the risk of  
31 violations from legislative effluent limits. As a result, these solutions are not readily accepted by  
32 operators and practitioners (Beraud, 2009). The application of available mathematical models is a  
33 potential alternative for wastewater engineers to evaluate the viability of their proposed  
34 optimization scenarios without harming the real systems. Several studies focused on model-based  
35 energy optimization of various wastewater treatment processes, including (Fikar et al., 2005; Kim  
36 et al., 2008; Leeuw et al., 1996). Fikar et al. (2005) and Leeuw et al. (1996) determined the optimal  
37 sequence of aeration cycles for conventional activated sludge systems with the use of dynamic and  
38 stochastic optimization algorithms, respectively. Kim et al. (2008) implemented the iterative  
39 dynamic programming (IDP) and activated sludge models (Henze et al., 2000) to optimize the  
40 nitrogen removal process in a sequencing batch reactor (SBR). Besides, several studies highlighted

1 the energy recovery potential through both chemical and thermal processes (Cano et al., 2015;  
2 Frijns et al., 2013; Funamizu et al., 2001). One of the main challenges of any optimization practice  
3 is the heterogeneity of objectives (Balku and Berber, 2006). An optimal or non-dominated solution  
4 should offer a trade-off between the economic and operational objectives in WWTPs. Finding this  
5 trade-off is the core of any optimization attempt.

6 The main limitation of the more widespread utilization of model-based optimization of WWTPs  
7 is data scarcity. High cost and demanding workload related to experimental data and adequate  
8 sampling campaigns make the data collection process an unpleasant necessity for managing  
9 stakeholders in modeling and optimization projects (Borzooei et al., 2016). Besides, irregular and  
10 deficient sensor maintenance and cleaning, which can lead to erroneous on-line measurements,  
11 can also reduce the amount of valid data (Martin and Vanrolleghem, 2014). For an accurate study  
12 of WWTPs' energy efficiency, several variables should be monitored continuously by the plant  
13 manager or a modeler, precisely due to their influence on efficiency trends. Hence, data scarcity is  
14 a common problem in WWTP modeling and energy optimization projects, which has been rarely  
15 addressed in scientific studies in this field.

16 This study proposes a stepwise approach for model-based energy optimization of the biological  
17 nutrient removal activated sludge system in the largest Italian WWTP, at Castiglione Torinese,  
18 considering data quality and quantity problems encountered during the project. Following a  
19 thorough assessment of the development and calibration of the model in a previous study  
20 (Borzooei et al., 2019), the impact of the solids retention time (SRT) on various parameters  
21 involved in the performance assessment criteria (PAC) is investigated. According to the obtained  
22 results, the non-dominated operational condition is proposed to increase the plant energy  
23 efficiency, resulting in economic savings and the simultaneous improvement of pollutant removal.

## 24 **2. Materials and methods**

### 25 **2.1 Castiglione Torinese WWTP**

26 The centralized Castiglione Torinese plant, located in the Northwest part of Italy, is  
27 the largest Italian WWTP. The plant has a daily operating capacity of 590,000 m<sup>3</sup> of urban  
28 wastewater, corresponding to an organic load of 2.1 million of equivalent inhabitants, with  
29 approximately 10-15% contribution of industrial discharges. Following the preliminary  
30 treatment (grit and sand removal), the pre-treated wastewater flows into four parallel  
31 wastewater treatment modules resembling Modified Ludzack-Ettinger (MLE) activated  
32 sludge systems with primary clarifiers. The boundary condition of the modeling project  
33 was defined considering the feasibility of controlling a few operational parameters during  
34 sampling time, financial, and functional limitations. The decision was made to focus the  
35 modeling project on half of the wastewater treatment module with the most stable  
36 operational conditions. Fig.1 demonstrates the schematic of a typical half-module in the  
37 Castiglione Torinese WWTP. Further details about the plant and operational details can be  
38 found in Borzooei et al. (2019).

39

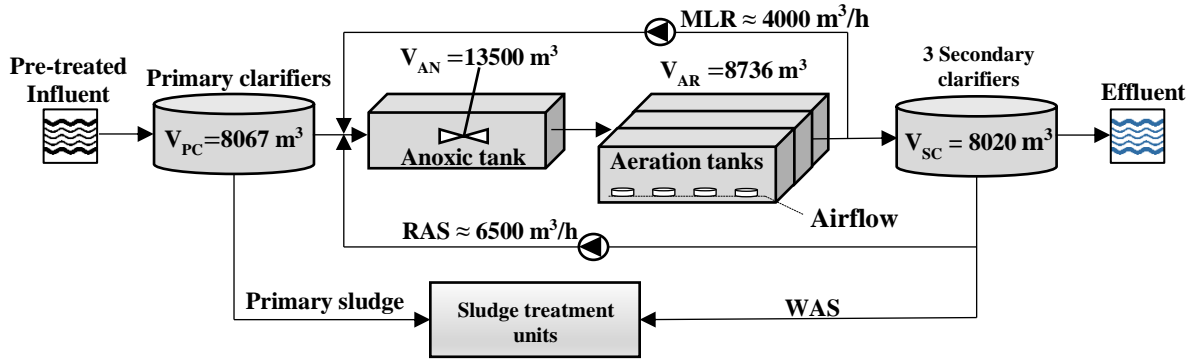


Fig. 1 The scheme of a typical wastewater treatment a half-module at Castiglione Torinese WWTP

## 2.2 Data collection

### 2.2.1 Sampling and measuring campaigns

The data collection was initiated with a collection of the routinely recorded data including, 24 h flow proportional composite samples from 2009 to 2016, physical characteristics of the treatment units, the design, and operational data. Following the analysis of the available data, field measurements were conducted to estimate internal mixed liquor recirculation (IMLR) and return activated sludge (RAS) flow rates. The COD fractionation of influent wastewater was performed according to the Dutch Foundation for Applied Water Research (STOWA) protocol (Hulsbeek et al., 2002). The daily composite samples were collected from the inlet and outlet of the half-module on four working days. Four main fractions, namely, readily ( $S_s$ ), slowly ( $X_s$ ) biodegradable COD, soluble ( $S_I$ ), and particulate ( $X_I$ ) inert COD, were identified. A detailed description of the fractionation along with justification of the minor modifications made to the original protocol can be found in Borzooei et al. (2019). Furthermore, an intensive 20-day sampling campaign, from September 26th to October 21st, 2016, was carried out for this study. The grab samples were collected from the inlet and outlet of each treatment unit. A lag time, according to the average hydraulic retention time (HRT) of the unit, was set between the two following sampling points. Samples were collected from RAS at a specific time during each day. Grab samples were further analyzed based on the IRSA methodology (IRSA, 1994) and the concentration of total COD (COD<sub>t</sub>), soluble COD (COD<sub>s</sub>), supernatant COD (COD<sub>sup</sub>), total suspended solids (TSS), total nitrogen (TN), ammonium (NH<sub>4</sub>) and nitrate (NO<sub>3</sub>) were measured. CODs was measured from the filtered and flocculated samples by 0.45µm filters and Zinc hydroxide [Zn (OH)<sub>2</sub>]. All available online measurements, including waste activated sludge (WAS) and primary sludge (PS) flow rates, were collected from the Supervisory Control and Data Acquisition (SCADA) system. The performance of sensors installed in the module was evaluated by grab sampling results as well as the real-time measurement with a portable device (Hach HQ30D portable meter). Finally, a 2-day composite sampling campaign with 2-hour intervals was conducted, in which samples were collected at the inlet and outlet of the half-module.



## 1 2.2.2 Electrical energy consumption

2 An inventory of all the electro-mechanical devices was made at an initial stage to obtain the energy  
3 consumption data. Using the plant tele-control system, all the main electro-mechanical instruments  
4 were included in the survey except for electrical valves, for which energy consumption was  
5 assumed negligible (Panepinto et al., 2016). Further, parameters such as power, voltage, and power  
6 factor were collected from the label of each electro-mechanical device. Operating time for each  
7 instrument was estimated by the use of the information available in SCADA and the data provided  
8 by technical staff. Digital Multimeter (Votcraft VC280) equipped with a current clamp (CLA-  
9 40VC200) was used to measure the current absorption ( $I_c$ ) of treatment units. Since the engines  
10 are three-phase systems, three measurements were conducted to estimate the  $I_c$  for each instrument.  
11 The absorbed power of each device ( $P$ ) was calculated according to *Eq.1*.

$$12 \quad P = \sqrt{3} \cdot V \cdot \bar{I}_c \cdot \cos \varphi \quad (\text{Eq.1})$$

13 where  $\bar{I}_c$  is the average of three  $I_c$  measurements,  $V$  is the voltage (set to 360 V), and  $\varphi$  is the power  
14 factor for each instrument. In a few cases,  $P$  was directly measured by the use of the ammeter  
15 (PCM1, PCE instruments).

16

## 17 2.3 Model development

18 In this study, a model was developed in the CN library of the wastewater treatment process  
19 simulator (GPS-X ver. 6.5.1) (Snowling, 2016) to mimic and simulate the removal of carbon and  
20 nitrogen components in the plant. Although chemical phosphorus removal is performed by dosing  
21 ferric chloride solution ( $\text{FeCl}_3$ ) into the RAS stream, it was excluded from modeled processes due  
22 to data scarcity. Hence, ASM1 was found as the best choice for the case of this study. The plant  
23 characteristics, including liquid temperature, blower inlet temperature, and site barometric  
24 pressure, were adjusted according to collected data. In the absence of tracer measurements, the  
25 “tanks-in-series” approach and an empirical formula proposed by (Murphy and Boyko, 1970) were  
26 employed to investigate the mixing regimes in aeration units. As a result, one continuous stirred-  
27 tank reactor (CSTR) was considered for each aeration unit and anoxic tank. An ideal, zero-  
28 dimensional, nonreactive clarifier model (removal efficiency by concentration) (Snowling, 2016)  
29 and a pre-compiled, one-dimensional flux dynamic, non-reactive secondary clarifier model  
30 (Takács et al., 1991) were implemented. For simplification purposes, three secondary clarifiers in  
31 the half-module were modeled as a single flat bottom circular clarifier with accumulated volume,  
32 with an assumption of an equal hydraulic load. Given that no data on settling parameters were  
33 available, the correlation model (Snowling, 2016) was implemented. The model implemented for  
34 this study includes three theoretical settling parameters in Vesilind, hindered, and flocculent zones,  
35 which are correlated to two intelligible parameters, namely, sludge volume index (SVI) and a  
36 clarification factor ( $c_f$ ). The sludge volume index links to the thickening function at the bottom of  
37 the clarifier, and clarification factor calibrates the clarification function (Snowling, 2016). The

1 reactive nature of secondary clarifiers was confirmed by nitrate removal (2 mg/l on average)  
 2 measured during the sampling campaign and modeled by placing a virtual anoxic CSTR in the  
 3 RAS stream. The volume of the virtual tank was defined as an estimated volume of the sludge  
 4 blanket, approximately 50% of VSC. Furthermore, all the available physical and operational  
 5 parameters were adjusted in the simulator according to the data obtained from the Castiglione  
 6 Torinese plant.  
 7 For modeling of the aeration system, the depth and volume of the basins as well as the physical  
 8 properties of the diffusers were adjusted, and the standard oxygen transfer efficiency (SOTE) of  
 9 each tank was calculated according to an empirical correlation proposed by (Hur, 1994):

$$10 \quad SOTE = A_1 + A_2 \cdot d_a + A_3 \cdot d_a^2 + A_4 \cdot d_d + A_5 \cdot d_{de} \quad (Eq.2)$$

11 where  $d_a$  is the airflow per diffuser,  $d_d$  is the diffuser submergence depth,  $d_{de}$  is the diffuser density  
 12 and  $A_1 - A_5$  are regression parameters. These regression parameters were obtained from an  
 13 extensive iterative adjustment and re-estimation process to reach the best fit of simulated and  
 14 recorded air flowrate. Finally, a proportional-integral (PI) controller was used to regulate the  
 15 airflow pumped to each basin based on dissolved oxygen (DO) measurements.  
 16 The delivered power blower ( $P_D$ ) in the aeration tanks was evaluated according to the adiabatic  
 17 compression equation (Mueller et al., 2002), as follows:

$$18 \quad P_D = \frac{wRT_a}{K} \left[ \left( \frac{P_d}{P_a} \right)^{\bar{K}} - 1 \right] \quad (Eq.3)$$

19 where  $w$  is the mass of the airflow,  $R$  is the universal gas constant ( $8.314 \text{ J}\cdot\text{mol}^{-1}\cdot\text{K}^{-1}$ ),  $T_a$  is the  
 20 blower inlet air temperature ( $^{\circ}\text{C}$ ) which was measured during the sampling period and  $\bar{K}$  is equal  
 21 to  $R/C_p$ , where  $C_p$  is the heat capacity of air at constant pressure. In this study,  $\bar{K}$  is assumed to be  
 22 0.283 based on U.S standard air.  $P_d$  is the discharge pressure of the blower (kPa), which was  
 23 calculated from Eq. 4:

$$24 \quad P_d = P_s + g \cdot d_d + \Delta P_d \quad (Eq.4)$$

25 where  $g$  is the gravity acceleration ( $9.81 \text{ m/s}^2$ ),  $\Delta P_d$  is the pressure drop of the piping and diffuser  
 26 downstream of the blower, and  $P_s$  is the barometric pressure. The absolute pressure upstream of  
 27 the blower (kPa) ( $P_a$ ) is the difference between  $P_s$  and pressure drop of the inlet filters and piping  
 28 of the blower ( $\Delta P_a$ ). Finally, the wire power consumed by the blowers to deliver the required air  
 29 ( $P_W$ ) was calculated by applying an overall efficiency coefficient for all mechanical equipment  
 30 used in the aeration system (i.e., blowers, motors, gearbox, etc.) ( $e$ ) according to Eq. 5.

$$31 \quad P_W = \frac{P_D}{e} \quad (Eq. 5)$$

32 The fixed speed pump model was implemented for modeling of the pumping systems in different  
 33 treatment units. The model can dynamically estimate the pumping head and efficiency by using  
 34 the pump characteristic curves under different flow rates. The required pumping head ( $H_s$ ) was

1 calculated by summing up the static head ( $H_{st}$ ), the actual lift between suction and discharge point,  
2 and the dynamic head ( $H_d$ ). The  $H_d$  was calculated from Eq.6:

$$H_d = K \cdot Q^2 \quad (Eq.6)$$

3  
4 where  $Q$  is the pumping flow rate, and  $K$  is the dynamic head-loss coefficient, which can be  
5 estimated by curve fitting exercised on a set of given  $Q$  and  $H_d$  values. The friction losses in  $H_d$   
6 are due to wastewater flow through the piping system, including valves and fittings (Amerlinck et  
7 al., 2012). As the last energetic contribution, the energy consumption of mechanical mixing  
8 operations was modeled by considering the power per unit mixing volume ( $P_{PUV}$ ) ( $\text{kW}/\text{m}^3$ )  
9 parameter. Additionally, the energy consumption of the external pumps and rakes working in  
10 secondary clarifiers was modeled as a constant miscellaneous power usage equal to 90 kWh/d.

## 11 12 **2.4 Model calibration**

13 An iterative, four-step calibration procedure (Borzooei et al., 2019) was implemented to  
14 fine-tune the model parameters. The most sensitive parameters were initially selected based  
15 on calibration protocols, full-scale observations, and sensitivity analysis, using a one-  
16 variable-at-a-time approach. These parameters were further adjusted by the use of the  
17 Nelder-Mead simplex (polyhedron) algorithm (Nelder and Mead, 1965) and following a  
18 specific order to compensate for the correlational effect of adjusted parameters on each  
19 other. In case of encountering any identifiability issues in parameter estimation phase in  
20 which more than one combination of model parameters would become a good fit for the  
21 observed data set, the realistic set of parameters was selected based on the project objectives  
22 and the plant practical conditions (Kristensen et al., 1998). Influent, biokinetic, primary,  
23 and secondary clarifier sub-models were calibrated by adjusting 11 parameters in the  
24 model. The aeration process was fine-tuned by adjusting the  $\alpha$  factors (ratio of process  
25 water to clean water mass transfer coefficients) to improve the fit between recorded and  
26 modeled DO and airflow data. Furthermore, a linear proportional-integral (PI) controller  
27 was implemented to regulate the airflow pumped to each basin based on the DO  
28 measurements. The controller was tuned by adjusting the DO setpoint, proportional gain  
29 ( $K_c$ ), and integral time ( $T_i$ ). Two parameters of the pressure drop in piping and diffuser  
30 downstream of the blower ( $\Delta P_a$ ) and the combined blower and motor efficiency ( $e$ ), were  
31 adjusted for calibration of the aeration energy model in three aeration units. Besides, the  
32 mixing energy consumption model in the anoxic tank was calibrated by tuning the  $P_{PUV}$ .  
33 Finally, to calibrate the pumping energy consumption models for the primary clarifier (PS  
34 pumping system), aeration units (IMLR pumping system) and the secondary clarifier (WAS  
35 and RAS pumping systems), pump efficiency ( $P_e$ ) and pipe friction loss ( $P_{FL}$ ) parameters  
36 were adjusted.

## 1 2.5 Performance assessment criteria

2 One of the main challenges for the optimization of WWTPs is defining a proper evaluation system,  
3 which contains all the essential and relevant indicators such as effluent quality, energy  
4 consumption, and greenhouse gas emissions. In this study, two types of effluent quality-based and  
5 energy-based performance assessment criteria (PAC) were considered. For the former type,  
6 average values and dynamic patterns of effluent COD, TSS, TN, N-NH<sub>4</sub>, N-NO<sub>3</sub>, and TKN  
7 concentrations were obtained following each simulation. In addition, the number of times and  
8 percentage of the time in which the effluent concentrations violated the effluent quality constraints  
9 were identified during the studied period. The effluent quality constraints of EU Directive  
10 91/271/EEC (EEC Council, 1991) were considered in this study. However, it should be noted that  
11 the Castiglione Torinese WWTP is following the limits of Italian environmental directives (e.g.  
12 D. lgs. 152/2006). Moreover, in real practice, the final effluent of each biological treatment  
13 module is sent to final filtration units, where it is divided over 27 multilayer sand and anthracite  
14 coal filtration units. To reduce the complexity of the modeling project and to focus this study on  
15 the optimization of the secondary treatment units only, both abovementioned issues were not  
16 considered. Hence, the real energy consumption and final effluent concentrations are, respectively,  
17 higher and lower in comparison to what is obtained in this study.

18 Furthermore, the instantaneous effluent quality index (EQI) and moving average effluent quality  
19 index (EQI<sub>a</sub>) (kg pollution per unit time) were estimated based on the expressions proposed in the  
20 COST simulation benchmark (Copp, 2002). The net instantaneous effluent quality index (EQI<sub>n</sub>)  
21 and moving average net effluent quality index (EQI<sub>n-a</sub>) (kg pollution per unit time) representing  
22 the weighted pollution load above the effluent limitations, were calculated based on Eq. 7 and 8:

$$23 \quad EQI_n = Q_e(t) \cdot \sum_{i=1}^n w_i \cdot \max[0, (C_i(t) - C_{i,limit})] \quad (Eq. 7)$$

$$24 \quad EQI_{n-a} = \frac{1}{T \cdot 1000} \int_t^{t+T} Q_e(t) \sum_{i=1}^n w_i \cdot \max[0, (C_i(t) - C_{i,limit})] \cdot d(t) \quad (Eq. 8)$$

25 where  $T$  is the period considered for the moving average calculation (d),  $Q_e(t)$  is the effluent flow  
26 rate time function (m<sup>3</sup>/d),  $n$  is the number of effluent quality parameters,  $C_i(t)$  and  $C_{i,limit}$  are the  
27 effluent concentration-time function (g/m<sup>3</sup>) and limits respectively, and  $w_i$  is the weight factor of  
28 the parameter  $i$ . Five effluent quality parameters ( $n = 5$ ), namely, BOD<sub>5</sub>, COD, TSS, TKN, and  
29 NO<sub>3</sub> were considered in estimating the effluent quality indexes. Corresponding weights were  
30 adopted from the extended version of Benchmark Simulation Model No.1 (Nopens et al., 2010),  
31 where the higher TKN weight factor ( $W_{TKN} = 20$ ) was proposed in comparison to NO<sub>3</sub> ( $W_{NO_3} =$   
32 10) to consider the higher ecological and toxicological impact for receiving water bodies of  
33 ammonia compared to nitrate (Camargo and Alonso, 2006).

34 The energy-based PAC contains estimations of the cumulative aeration ( $E_{Ca}$ ), mixing ( $E_{Cm}$ ),  
35 pumping ( $E_{Cp}$ ), and total energy consumption ( $E_{Ct}$ ) in the simulation period. Besides, the amount  
36 of total energy produced from WAS ( $E_{Pw}$ ) was estimated following the stepwise procedure  
37 presented in Fig. 2.

38

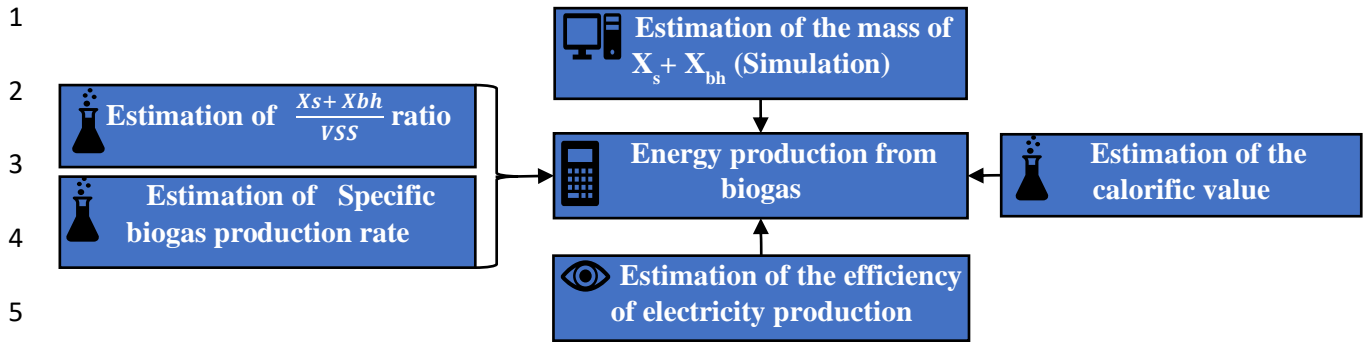


Fig. 2 Stepwise procedure for estimating the energy production from waste activated sludge (WAS)

It should be noted that primary sludge (PS) was excluded from this methodology since, in the SRT scenario analysis (see section 2.6), PS flow pattern was constant. The proposed methodology hypothesizes that the biogas production from the WAS is directly linked to the amount of  $X_s$  (slowly biodegradable substrate) and  $X_{bh}$  (active heterotrophic biomass) fractions since they are the primary biodegradable sources of COD in WAS (Martinello, 2013). An equal biodegradability between  $X_{bh}$  and  $X_s$ , and complete hydrolysis and transformation of  $X_{bh}$  into  $X_s$  in the sludge treatment process were assumed in the methodology.

In the first step, the total mass of  $X_s+X_{bh}$  ( $M_x$ ) was measured for the simulation time. Furthermore, in order to estimate the specific biogas production rates, results presented in (Ruffino et al., 2015) were implemented. (Ruffino et al., 2015) investigated the performance of mechanical and low-temperature thermal pre-treatments for improving the efficiency of anaerobic digestion carried out on WAS of the Castiglione Torinese WWTP. It obtained specific biogas production rates of untreated samples between 0.234 and 0.263  $Nm^3/KgVS$ .

Therefore, the specific biogas production rate of 0.25  $Nm^3/KgVSS$  was considered in this study. Likewise, a  $X_s/VSS$  ratio of 1.42 was assumed, as reported in (Takács and Vanrolleghem, 2006). The same ratio can be applied for  $X_{bh}$ , considering the complete hydrolysis assumption. The specific gas production was calculated as 0.355  $Nm^3$  biogas/kg ( $X_s+X_{bh}$ ). A calorific value equal to 6.25  $kWh/m^3$  (Banks, 2009), and 42 % of electricity production efficiency were assumed in this study. Finally, the produced energy from biogas was calculated from Eq. 9.

$$E_{Pw}(kWh) = M_x \times \frac{0.355 Nm^3 biogas}{kg(X_s+X_{bh})} \times \frac{6.25 kWh}{Nm^3} \times 0.42 \quad (Eq. 9)$$

For each simulation period, an accumulated  $E_{Pw}$  was calculated and reduced from  $E_{Ct}$  to obtain total net energy consumption ( $E_{Cn}$ ).

## 2.6 Process optimization

The SRT or mean cell retention time (MCRT) represents the time that microorganisms remain in the system and reproduce or regenerate. Given that various types of microorganisms have distinct regeneration times, the SRT duration can play a significant role in their proliferation or washing out of the system. SRT is usually considered to be the main control parameter in biological wastewater treatment systems. Conducting a model-based investigation to measure the impact of

1 changing SRT on existing WWTP performance is an alternative that is less demanding in terms of  
2 time, costs, safety, and speed in comparison to real-world practice. Several model-based  
3 optimization attempts have been reported finding the optimum value for the SRT in operating AS  
4 systems (Coen et al., 1998; Salem et al., 2002).

5 In this study, a PI controller was added to the calibrated model in order to control the SRT around  
6 a pre-defined value by manipulating the WAS flow rate. Several dynamic simulations were  
7 conducted under various SRT values (10, 15, 20, 25, 30, 35, and 40 days). According to real plant  
8 experience, it takes around 3-4 SRTs for a WWTP to respond to any changes in operational  
9 parameters (Dotro et al., 2017). Therefore, to reduce the impact of initial conditions and obtain  
10 realistic simulation results, steady-state simulations were conducted for 100 days (3 times the  
11 average SRT in the ongoing plant operational condition) with each modified SRT value. The  
12 obtained results and concentrations from the steady-state runs were further used as the initial  
13 conditions for the dynamic simulations.

14 The proportional relation between SRT and oxygen transfer efficiency (OTE) in aeration units,  
15 related to the degree of treatment and removal of oxygen transfer reducing contaminants (e.g.,  
16 surfactants) were first reported in EPA (1989). In this study, given that no information about OTEs  
17 on aeration units was available, it was decided to estimate the impact of SRT on  $\alpha$  values using the  
18 empirical relations reported in Rosso et al. (2005). Analyzing the data sets collected from 372  
19 different flux-averaged off-gas measurements in 30 plants in the United States for 15 years, Rosso  
20 et al. (2005) reported statistical relations among various types of diffusers, aeration tank  
21 geometries, airflow rates, SRT and OTE. Firstly, for each aeration unit, normalized air flux ( $Q_N$ )  
22 was estimated from *Eq. 10*.

$$23 \quad Q_N = \frac{Q_a}{D_A \cdot N_D \cdot Z} \quad (\text{Eq. 10})$$

24 where  $Q_a$  is the airflow rate in aeration units ( $\text{m}^3/\text{s}$ ),  $D_A$  is a diffuser specific area ( $\text{m}^2$ ),  $N_D$  is the  
25 number of diffusers in aeration unit, and  $Z$  is diffuser submergence (m). Secondly, considering the  
26 average SRT of the studied module (SRT  $\approx 30$  d), the  $\alpha$  value ( $\alpha_e$ ) was estimated from linear  
27 logarithmic functions proposed in (Rosso et al., 2005). The  $\alpha_e$  values were further compared with  
28 numerically calibrated  $\alpha$  values ( $\alpha_c$ ) (see section 2.4), and three correction factors ( $F_c$ ) were  
29 introduced accordingly. Finally, assuming the same  $Q_N$  value, the corrected  $\alpha$  values ( $\alpha_{c0}$ ) were  
30 calculated by multiplying the  $\alpha_e$  by  $F_c$  for each SRT scenario. Following the abovementioned  
31 procedure, several dynamic simulations were performed under different SRT scenarios and results  
32 were compared in terms of parameters in the PAC. Fig.3 shows a comprehensive overview of the  
33 methods implemented in this study.

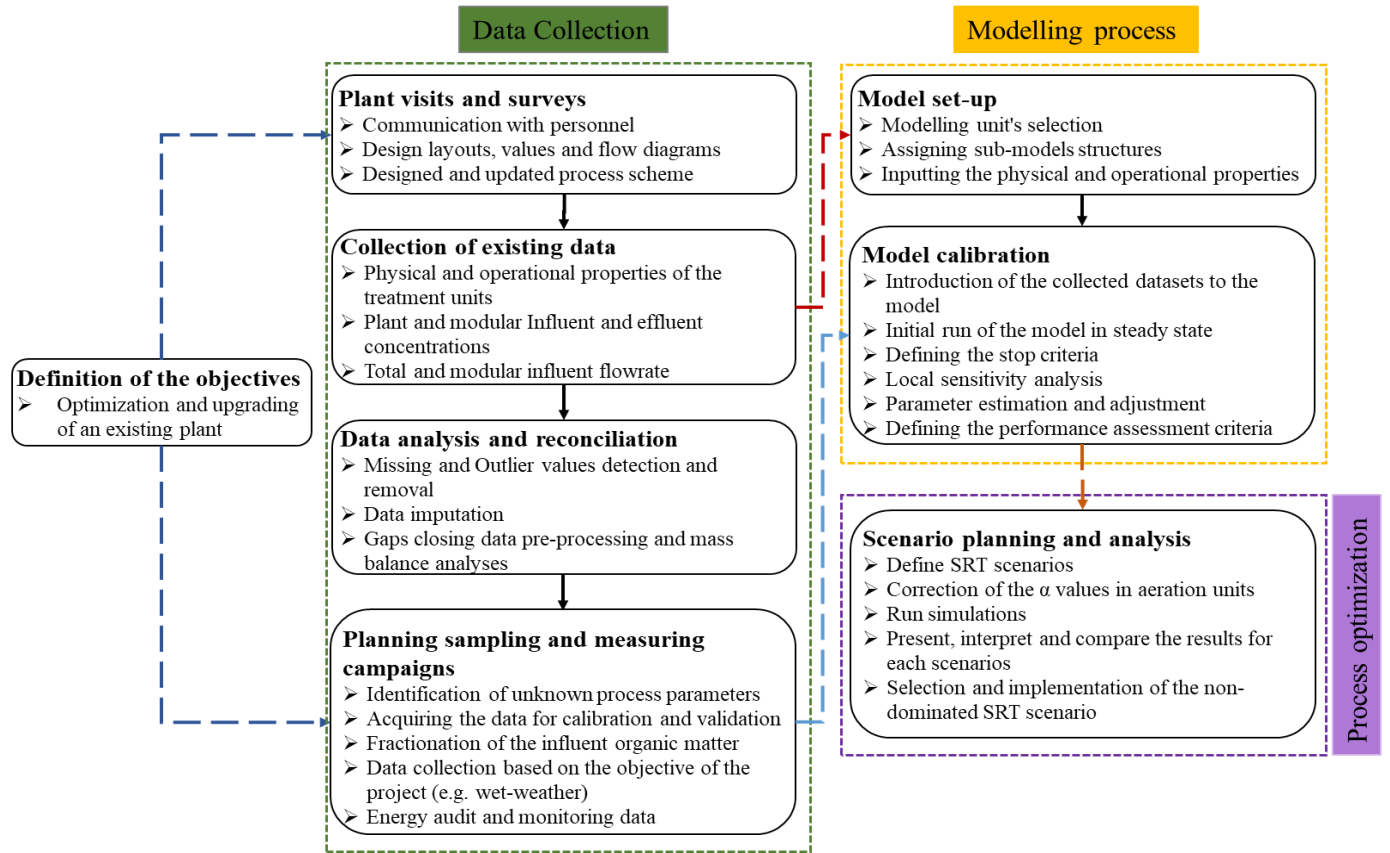


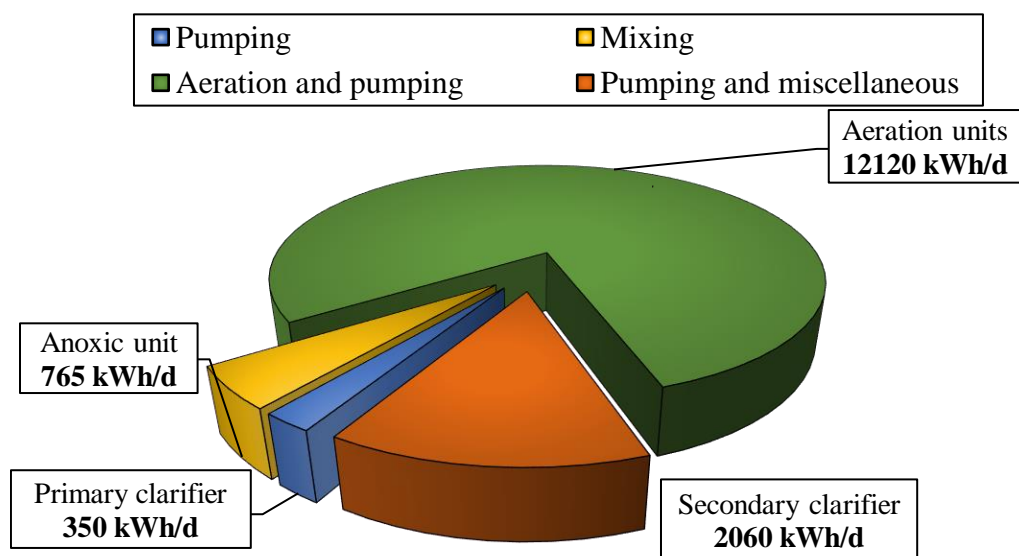
Fig. 3 A comprehensive schematic of methods implemented in this study

### 3. Results and discussion

#### 3.1 Data collection and practical challenges

An irregular discharge of reject water from sludge treatment units (RWS) into the studied half-module, as well as two extreme wet-weather events, occurred during the period of sampling campaign. Therefore, the dataset was partitioned into two main periods: 11-days normal operating conditions in dry weather (NC-D) and 9-days high load operating conditions in wet weather (HC-W), in which a discharge of RWS and a massive rain event occurred. During the 2-day dynamic sampling campaign, the discharge of RWS was recorded in dry weather conditions (HC-D). Partitioned results highlighted that the influent concentrations recorded in NC-D were almost doubled or tripled in HC-D operational mode. Moreover, the dilution effect of a wet-weather event on influent concentrations was observed, comparing the results recorded in HC-D and HC-W modes. Due to the high deviation of influent concentrations in various operational modes, the data collected in the NC-D was further elaborated for performance investigation of the treatment units (Borzooei et al., 2017) and model calibration (Borzooei et al., 2019). Performing measurements of primary sludge flow rate and its pumping energy have proved to be a challenging task, given that the only available relevant data were the sludge levels in the repository sumps and the on/off

1 patterns of two automated and modulating control valves sending the sludge to the corresponding  
 2 pre-thickeners. The flowmeter was installed at the entrance of a receiving pre-thickener to measure  
 3 the amount of primary sludge entering the system. However, the number of active pre-thickeners,  
 4 their capacities, number of receiving pre-thickeners, both primary and secondary sludge, as well  
 5 as the corresponding pre-thickeners of each primary clarifier, were changing continuously during  
 6 the operational period of the plant. Finally, operators were updated and instructed to keep  
 7 operational parameters constant during the period of the sampling campaign.  
 8 While studying the pumping patterns of the WAS during the sampling period, it was found that  
 9 the WAS flow rate was regularly changed by operators based on the functional capacity of pre-  
 10 thickeners in sludge treatment lines; as a result, its pumping pattern was changed on an hourly  
 11 basis. To calculate the SRT of the system, the average WAS flow rate was considered; however,  
 12 for the model development and calibration, the dynamic patterns were considered instead.  
 13 Furthermore, a discrepancy between grab sampling results and available DO and NH<sub>4</sub> sensor  
 14 readings due to sensor failure were observed in the aeration units. Dead zones, floating sludge, and  
 15 coarse bubbles or bulk air emission were observed on the surface of the aeration tanks caused by  
 16 diffusers' relocation, fouling, and membrane overstretching and/or tearing. Both issues and their  
 17 impacts on model development and calibration processes were addressed in detail in Borzooei et  
 18 al. (2019). The energy consumption of each treatment unit was estimated by multiplying the  
 19 calculated power (P) from Eq.1 to its operating time. The electro-mechanical equipment and  
 20 operating devices were further grouped and classified in homogeneous categories. The results of  
 21 the energy audit are provided in Fig. 4.



22  
 23 **Fig. 4 Energy audit data Energy Consumption the wastewater treatment module at Castiglione Torinese WWTP**

24 As seen in Fig. 4, the highest fraction of energy uptake is in the aeration process in biological  
 25 oxidation units (over 75%), followed by pumping and operational energy consumption in the  
 26 secondary clarifiers. Considering the high-energy use of aeration units, significant energy saving



1 can be obtained by operating the aeration system to match as closely as possible the real oxygen  
2 demand of the process. This highlights the importance of finding the optimum SRT on the energy  
3 consumption of the WWTP.

### 4 **3.2 Model calibration and simulation**

5 The model was calibrated under dynamic conditions with the data originating from both  
6 laboratory and sensor readings collected in the NC-D operational mode following the  
7 approach presented before. The initial fractions of organic matter in the influent wastewater  
8 were identified following the standard Dutch guidelines (Roeleveld and Van Loosdrecht,  
9 2002). The average contribution of individual ASM1 components to total COD was found  
10 as follows:  $S_I = 1.1\%$ ,  $S_s = 9.1\%$ ,  $X_s = 44\%$ ,  $X_I = 45.8\%$ . A total number of 8 model  
11 parameters were adjusted to calibrate influent, aeration, clarification, and biokinetic sub-  
12 models. After modifying the results obtained from the COD fractionation method, the  
13 influent model was cali

14 brated by increasing particulate COD (XCOD) to VSS ratio, based on the measurement of  
15 the  $COD_t$  and MLVSS in the aeration tanks. The primary clarifier model was calibrated by  
16 the reduction of the removal efficiency coefficient from its default value.

17 Secondary clarifiers were calibrated by adjusting  $C_c$  and SVI based on TSS concentration  
18 measured at final effluent and RAS, respectively. Further, assuming the fouling factor ( $F_f$ )  
19 equal to 1, aeration models were calibrated by adjusting  $\alpha$  values to obtain the best fit  
20 between measured and modeled DO and airflow rate at each aeration unit. Finally, the  
21 maximum specific growth rate for autotrophic biomass ( $\mu_A$ ), oxygen half-saturation index  
22 for autotrophic biomass ( $K_{OA}$ ), and autotrophic decay rate ( $b_A$ ) were adjusted to calibrate  
23 biokinetic models. Details about the calibration practice can be found in (Borzooei et al.,  
24 2019). The results of sensitivity analysis in the calibration of pumping energy consumption  
25 sub-models showed almost the same amount of sensitivity for both pump efficiency ( $P_e$ )  
26 and pipe friction loss ( $P_{FL}$ ) in two different pumping units considered in the model.

27 Consequently, since no practical information was available about both parameters, one of  
28 the obtained combinations in the parameter estimation process was selected based on  
29 engineering judgment.

30 On the other hand, in the calibration of the aeration energy models, combined blower and  
31 motor efficiency ( $e$ ) carried a stronger influence than the pressure drop in piping and  
32 diffuser downstream of the blower ( $\Delta P_a$ ), as a result initially the  $e$  parameter was adjusted  
33 followed by  $\Delta P_a$ . Adjusted energy-related parameters and the modeling results are tabulated  
34 in Table 1. Comparing the energy audit and simulation results, it can be observed that model  
35 predictions are in relatively good agreement with energy audit data.

36  
37  
38  
39  
40

1

Table 1. Adjusted energy-related parameters and modeling results in the calibration process

Parameter definition	Symbol	unit	value
<b>Pumping energy</b>			
Pump efficiency primary clarifier	$P_{e,P}$	-	0.12
Pipe friction loss primary clarifier	$P_{FL,P}$	m	25
Pump efficiency of IMLR	$P_{e,MLR}$	-	0.65
Pipe friction loss of IMLR	$P_{FL,MLR}$	m	6
Pump efficiency of WAS	$P_{e,WAS}$	-	0.2
Pipe friction loss of WAS	$P_{FL,WAS}$	m	10
Pump efficiency of RAS	$P_{e,RAS}$	-	0.4
Pipe friction loss of RAS	$P_{FL,RAS}$	m	2.5
<b>Mixing energy</b>			
Power per unit volume for aeration tanks	$P_{PUV,Ar}$	W/m <sup>3</sup>	0.01
Power per unit volume for the anoxic tank	$P_{PUV,An}$	W/m <sup>3</sup>	2.5
<b>Aeration energy</b>			
Pressure drop in piping and diffuser Downstream of blower for 3 aeration units	$\Delta P_a$	atm	0.08
Combined blower and motor efficiency	$e$	-	0.25
<b>Pumping energy in primary clarifier</b>	-	kWh/d	369
<b>Mixing energy in Anoxic tanks</b>	-	kWh/d	810
<b>Aeration and pumping energy in aeration units</b>	-	kWh/d	13138
<b>Pumping and miscellaneous energy in secondary clarifiers</b>	-	kWh/d	1988
<b>Total energy consumption</b>	$E_{Ct}$	kWh/d	16305

2

### 3.3 Model-based process optimization

Several dynamic simulations were performed under various SRT values (10, 15, 20, 25, 30, 35, and 40 days). To estimate the impact of various SRTs on the  $\alpha$  values, the statistical relation reported in Rosso et al. (2005) was used. For three aeration units, a normalized air flux ( $Q_N$ ) and estimated  $\alpha$  ( $\alpha_e$ ) were calculated. Comparing the calibrated  $\alpha$  ( $\alpha_c$ ) with  $\alpha_e$  values, three correction factors ( $F_c$ ) were identified. The results are tabulated in Table 2.

9

10

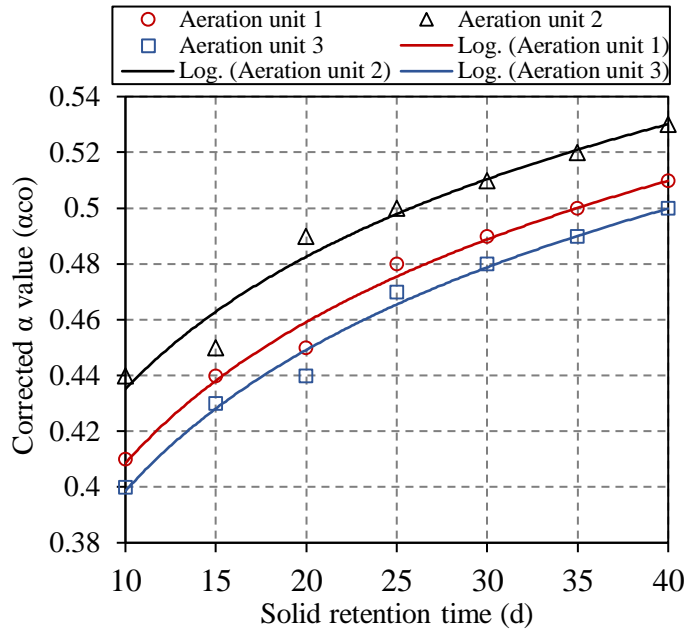
Parameter	Aeration unit 1	Aeration unit 2	Aeration unit 3
$\alpha_c$	0.49	0.51	0.48
$Q_N$	0.00126	0.00102	0.00127
$\alpha_e$	0.63	0.64	0.63
$F_c$	0.78	0.79	0.76

11

Finally, assuming the same  $Q_N$  value, corrected  $\alpha$  ( $\alpha_{Co}$ ) values were calculated by multiplying the  $\alpha_e$  by  $F_c$ . Obtained  $\alpha_{Co}$  values of aeration units for SRT scenarios are

13

1 demonstrated in Fig. 5. To better illustrate the  $\alpha_{Co}$  values' trend, logarithmic best-fit curved  
 2 lines were used, as shown in Fig. 5.



3

4 **Fig. 5 The Corrected ratio of process water to clean water mass transfer coefficients ( $\alpha$ ) for various SRTs**

5 After adjusting the  $\alpha$  values in the calibrated model, a series of dynamic simulations were  
 6 performed under various SRT scenarios and all PAC parameters were identified. Following each  
 7 simulation, average values and dynamic patterns of effluent COD, TSS, TN, N-NH<sub>4</sub>, N-NO<sub>3</sub>, and  
 8 TKN concentrations were investigated. Box-and-whisker plots of TSS, COD, NH<sub>4</sub> and NO<sub>3</sub>  
 9 effluent concentrations were examined for each SRT scenario (Fig. 6). The upper and lower boxes  
 10 show the locations of the first and third quartiles (Q<sub>1</sub> and Q<sub>3</sub>) and the lines across the box represent  
 11 the mean. The whiskers lines represent the range between the lowest and highest observations in  
 12 the region defined by Q<sub>1</sub> - 1.5 (Q<sub>3</sub> - Q<sub>1</sub>) and Q<sub>3</sub> + 1.5 (Q<sub>3</sub> - Q<sub>1</sub>). For clarity purposes, the limited  
 13 number of individual points with values outside this range were not plotted.

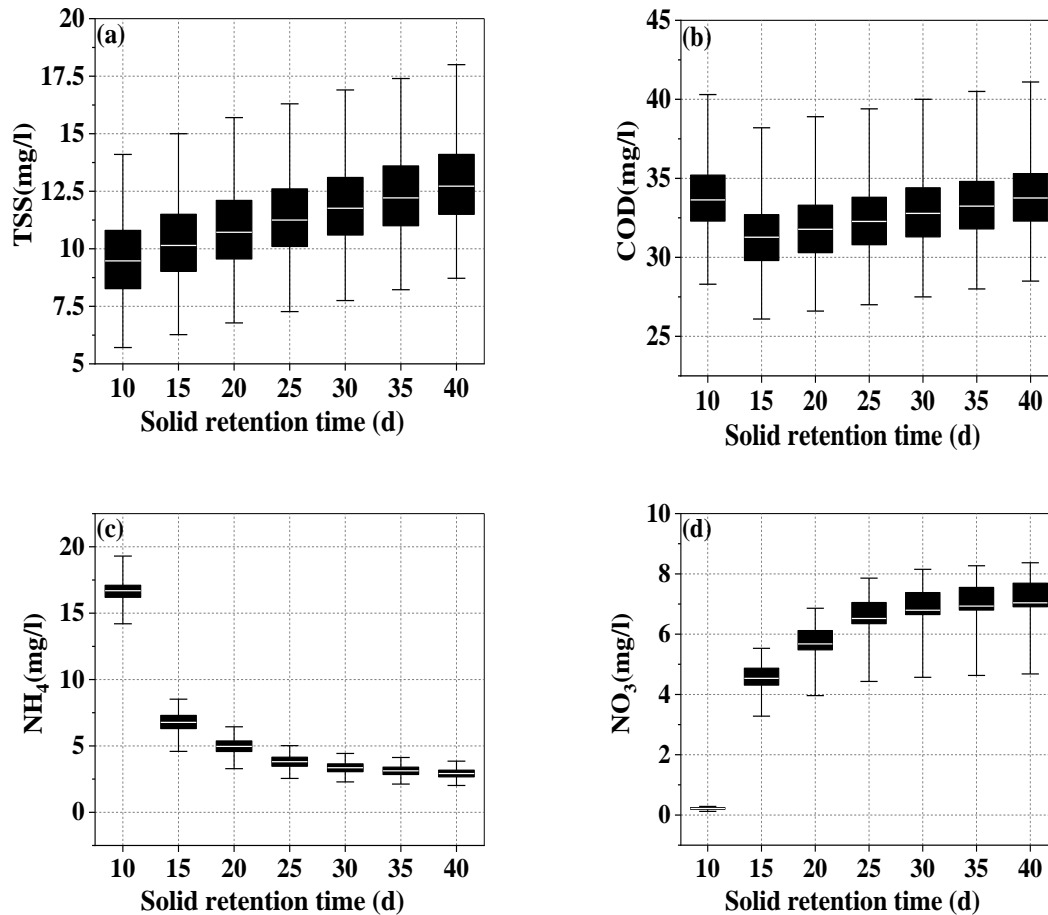


Fig. 6 Variations of TSS (a), COD (b), NH<sub>4</sub> (c) and NO<sub>3</sub> (d) effluent concentrations

1  
2  
3

4 Investigating the mean values (white lines) in Fig. 6(a), a gradually rising trend of effluent  
5 TSS can be observed. Since SRT was controlled by manipulating the WAS flow rate,  
6 increasing the SRT causes a higher MLSS in the aeration units, hence higher TSS  
7 concentration in the effluent. The mean values of effluent COD concentration presented in  
8 Fig. 6 (b), show a slightly dropping COD by increasing SRT from 10 to 15 days (due to  
9 oxidation and biodegradation of available biodegradable COD under the presence of  
10 enough DO) and by net growth of microorganisms (as a result of increasing SRT and halting  
11 biomass washout, which occurs in SRT of 10 days).

12 However, increasing SRT from 15 to 40 days raises the amount of biomass present in the system  
13 (though with lower growth rates) while the amount of available soluble substrate reaches its  
14 minimum plateau stage. The upward trend of COD after SRT of 15 days can be attributed mainly  
15 to the loss of active biomass and/or cell debris as particulate biodegradable and/or inert COD,  
16 which occurs due to higher MLSS and SRT. In addition, it should be noted that increasing the SRT  
17 produces a decline in the system's substrate concentration and lower substrate utilization rate.

1 Studying the variation of average effluent  $\text{NH}_4$  and  $\text{NO}_3$  concentrations in Fig. 6(c) and (d), three  
2 phases can be identified. In the first phase, the sharp decline of  $\text{NH}_4$  and steep rise of  $\text{NO}_3$   
3 concentration are observed by increasing the SRT value from 10 to 15 days. Due to the high flow  
4 WAS rate under SRT of 10 days, nitrifier microorganisms are washed out at a faster rate than they  
5 regenerate; as a result, incomplete or no nitrification occurs. Consequently, the mean effluent  $\text{NO}_3$   
6 obtained in SRT=10 days is in high agreement with measured values during the sampling  
7 campaign. Further prolonging SRT from 15 to 20 days, nitrification is initiated through which  
8 ammonia is consumed, and nitrate is produced. Since the contrast between these two operational  
9 conditions is significant, steep slopes are obtained in this phase. Consequently, SRT =15 days is  
10 detected as the minimum operational condition for nitrification in the system.

11 In the second phase, a moderate decline of  $\text{NH}_4$  and an increasing slope of  $\text{NO}_3$  can be observed  
12 moving from SRT of 15 to 25 days. Due to increasing the residence time from the minimum SRT  
13 value for nitrification, nitrogen species are oxidized by nitrifying bacteria remaining in the aeration  
14 system for the period equal or slightly more than their regeneration time. As a result, ammonia  
15 oxidization occurs with an almost dropping rate (substrate utilization rate decreases with  
16 increasing of SRT).

17 In the third phase, a mild declining slope of  $\text{NH}_4$  and a mild increasing slope of  $\text{NO}_3$  concentrations  
18 from SRT= 25 to 40 days can be identified. The slightly declining trend of effluent nitrogen species  
19 can occur due to the increased residence time from 25 days, which provides nitrifying bacteria a  
20 higher residence time than their regeneration time. However, soluble substrates will reach their  
21 minimum plateau and be depleted with increasing the SRT. As a result, biomass concentration  
22 may gradually decrease in this phase due to microorganism decay.

23 Finally, cumulative moving average net effluent quality index ( $\text{EQI}_{n-m}$ ), total energy consumption  
24 ( $E_c$ ), and daily averaged energy production from waste activated sludge ( $E_{pw}$ ) were obtained from  
25 the results of the simulations under each SRT scenario. For the simulation period, a cumulative  $E_{pw}$   
26 was calculated and reduced from  $E_{ct}$  to obtain total net energy consumption ( $E_{cn}$ ). Fig. 7  
27 demonstrates a comparison of SRT scenarios in terms of cumulative effluent quality and energy  
28 consumption in the simulation period.

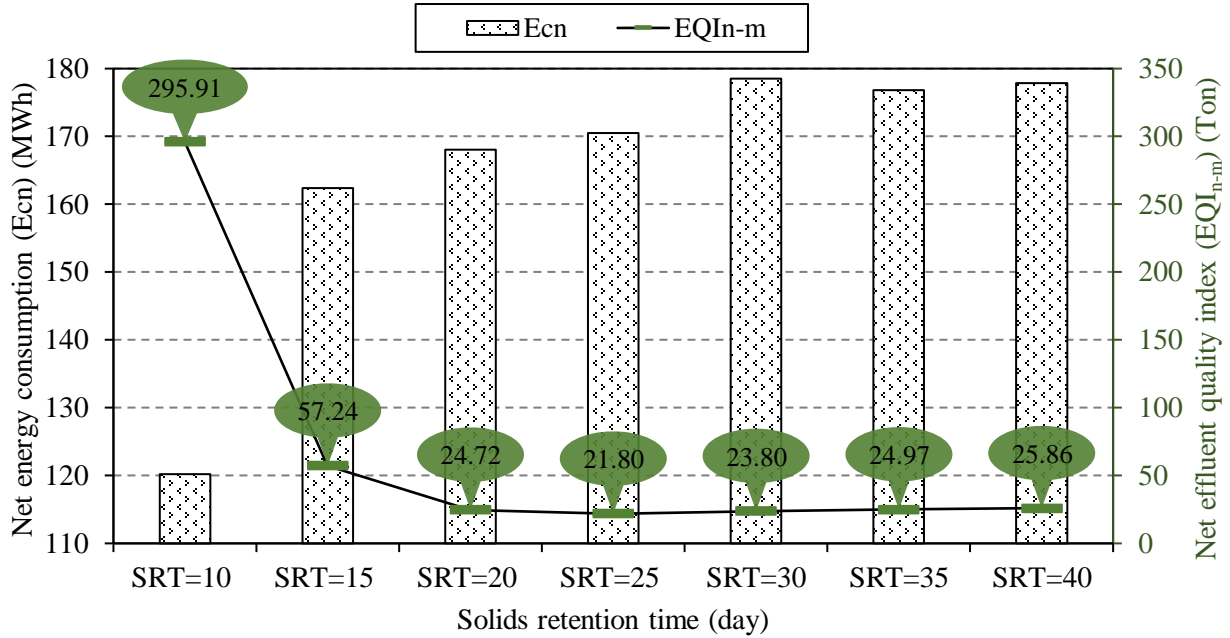


Fig. 7 Energy-based and effluent quality parameters in PAC obtained under various SRT scenarios

Fig. 7 highlights that the minimum  $EQI_{n-m}$  was obtained from the model simulation under SRT of 25 days, whereas the minimum  $E_{c-n}$  was observed in the model with SRT of 10 days because of its high biogas production and low aeration energy. Considering the minimum obtained  $EQI_{n-m}$  under the SRT of 25 days and lower  $E_{c-n}$  compared to other scenarios, the setup was selected as a non-dominated operational scenario. Based on the sampling results and audited energy data, the Castiglione Torinese WWTP consumes 0.3 kWh for treating 1 m<sup>3</sup> of the influent wastewater in its current operation. The energy consumption of WWTPs is highly influenced by operational and environmental characteristics, such as pollutant loads, plant size, and age, as well as the type of WWTP (Venkatesh and Brattebø, 2011). Average energy consumption rates of WWTPs in Germany, United Kingdom, and the United States were reported as 0.67, 0.64, and 0.45 kWh/m<sup>3</sup>, respectively, while ranges for Italian WWTPs were reported between 0.40 to 0.70 kWh/m<sup>3</sup> (Cantwell, 2015; Guerrini et al., 2017). Applying the proposed operational modification in Castiglione Torinese, energy consumption could be reduced to almost 0.28 kWh/m<sup>3</sup>. This operational change could result in 5000 MWh savings of annual energy consumption, which is approximately equivalent to the annual residential electricity consumption of 1000 people in Italy (Eurostat, 2013).

#### 4. Conclusion

With the EU setting an ambitious energy efficiency target of 20% by 2020, energy monitoring and saving became a crucial task for managing wastewater treatment plants (WWTP). In response to this pressing requirement, this study proposed a robust methodology to develop and link energy consumption sub-models to wastewater treatment process model, with the use of limited energy audit data. The methodology proposed within this study was implemented for the case of the largest Italian WWTP. Several sub-models including biokinetic, aeration, hydraulic and transport,

1 clarifier, influent, and effluent in addition to energy consumption sub-models (aeration, pumping,  
2 and mixing), were developed and calibrated. A scenario-based optimization approach was carried  
3 out to adjust the critical operational parameter and optimize the performance of the WWTP.  
4 Effluent quality-based and energy-based performance assessment criteria (PAC) were considered  
5 to investigate the results of the simulations. The main trade-off between energy consumption and  
6 nutrient discharges could be optimally identified in the scenario with a solids retention time (SRT)  
7 equal to 25 days. The results demonstrate the promising potential of significant reductions in  
8 energy consumption of up to 5000 MWh, by improving effluent quality (8-10% reduction of the  
9 effluent quality index) through operational changes only. An inherent advantage of the  
10 methodology described in this paper is the capability of analyzing “what-if” scenarios, including  
11 performance optimization under extreme climatic events.

12

## 13 **5. Future directions**

14 This study can be further continued by investigating other plant operational modes (e.g., high load  
15 conditions due to the discharge of reject water from sludge units and wet-weather events) to  
16 propose more practical optimization scenarios for the plant operators. Furthermore, in response to  
17 legislative targets in the 2020 Climate and Energy Package, indicating a 20 % reduction in EU  
18 greenhouse gas (GHG) emissions, the application of new performance assessment criteria related  
19 to anthropogenic GHG emissions can be considered. To this end, a more comprehensive modeling  
20 library, containing sub-models mimicking emission of carbon dioxide (CO<sub>2</sub>), methane (CH<sub>4</sub>), and  
21 nitrous oxide (N<sub>2</sub>O) gases in various wastewater and sludge treatment processes, can be used.

22

## 23 **6. Acknowledgments**

24

25 This research was financially supported by Società Metropolitana Acque Torino (SMAT). The  
26 authors wish to thank SMAT managing, laboratory, maintenance, and operation personnel for their  
27 engagement and cooperation during the sampling campaigns of this project.

28

29

30

31

32

33

34

## 1 **References**

- 2 Amerlinck, Y., Bellandi, G., Amaral, A., Weijers, S., Nopens, I., 2016. Detailed off-gas  
3 measurements for improved modelling of the aeration performance at the WWTP of  
4 Eindhoven. *Water Sci. Technol.* 74, 203–211.
- 5 Amerlinck, Y., De Keyser, W., Urchegui, G., Nopens, I., 2012. Realistic dynamic pumping energy  
6 models for wastewater applications. *Proc. Water Environ. Fed.* 2012, 4140–4156.
- 7 Balku, S., Berber, R., 2006. Dynamics of an activated sludge process with nitrification and  
8 denitrification: Start-up simulation and optimization using evolutionary algorithm.  
9 *Comput. Chem. Eng.* 30, 490–499.
- 10 Banks, C., 2009. Optimising anaerobic digestion: Evaluating the Potential for Anaerobic Digestion  
11 to provide Energy and Soil amendment. *Univ. Read.* 39.
- 12 Bellandi, G., Porro, J., Senesi, E., Caretti, C., Caffaz, S., Weijers, S., Nopens, I., Gori, R., 2018.  
13 Multi-point monitoring of nitrous oxide emissions in three full-scale conventional activated  
14 sludge tanks in Europe. *Water Sci. Technol.* 77, 880–890.
- 15 Beraud, B., 2009. Methodology for the optimization of wastewater treatment plant control laws  
16 based on modeling and multi-objective genetic algorithms (PhD Thesis). Université  
17 Montpellier II-Sciences et Techniques du Languedoc.
- 18 Borzooei, S., Amerlinck, Y., Abolfathi, S., Panepinto, D., Nopens, I., Lorenzi, E., Meucci, L.,  
19 Zanetti, M.C., 2019. Data scarcity in modelling and simulation of a large-scale WWTP:  
20 Stop sign or a challenge. *J. Water Process Eng.* 28, 10–20.
- 21 Borzooei, S., Zanetti, M., Genon, G., Ruffino, B., Godio, A., Campo, G., Panepinto, D., Lorenzi,  
22 E., De Ceglia, M., Binetti, R., 2016. Modelling and calibration of the full scale WWTP  
23 with data scarcity, in: *Proceedings of International Symposium on Sanitary and*  
24 *Environmental Engineering, Rome.*
- 25 Borzooei, S., Zanetti, M.C., Lorenzi, E., Scibilia, G., 2017. Performance investigation of the  
26 primary clarifier- Case study of castiglione torinese, in: *Lecture Notes in Civil Engineering.*  
27 pp. 138–145. [https://doi.org/10.1007/978-3-319-58421-8\\_21](https://doi.org/10.1007/978-3-319-58421-8_21)
- 28 Caivano, M., Bellandi, G., Mancini, I.M., Masi, S., Brienza, R., Panariello, S., Gori, R., Caniani,  
29 D., 2017. Monitoring the aeration efficiency and carbon footprint of a medium-sized  
30 WWTP: experimental results on oxidation tank and aerobic digester. *Environ. Technol.* 38,  
31 629–638.
- 32 Camargo, J.A., Alonso, Á., 2006. Ecological and toxicological effects of inorganic nitrogen  
33 pollution in aquatic ecosystems: a global assessment. *Environ. Int.* 32, 831–849.
- 34 Cano, R., Pérez-Elvira, S.I., Fdz-Polanco, F., 2015. Energy feasibility study of sludge  
35 pretreatments: a review. *Appl. Energy* 149, 176–185.
- 36 Cantwell, J.C., 2015. Overview of State Energy Reduction Programs and Guidelines for the  
37 Wastewater Sector. *Water Intell. Online* 9. <https://doi.org/10.2166/9781780403397>
- 38 Coen, F., Petersen, B., Vanrolleghem, P.A., Vanderhaegen, B., Henze, M., 1998. Model-based  
39 characterisation of hydraulic, kinetic and influent properties of an industrial WWTP. *Water*  
40 *Sci. Technol.* 37, 317–326.
- 41 Copp, J.B., 2002. The COST Simulation Benchmark: Description and Simulator Manual: a  
42 Product of COST Action 624 and COST Action 682. EUR-OP.
- 43 Descoins, N., Deleris, S., Lestienne, R., Trouvé, E., Maréchal, F., 2012. Energy efficiency in waste  
44 water treatments plants: Optimization of activated sludge process coupled with anaerobic  
45 digestion. *Energy* 41, 153–164.



- 1 Dotro, G., Langergraber, G., Molle, P., Nivala, J., Puigagut, J., Stein, O., von Sperling, M., 2017.  
2 Treatment Wetlands. *Water Intell. Online* 16, 9781780408774.  
3 <https://doi.org/10.2166/9781780408774>
- 4 EEC Council, 1991. Council Directive 91/271/EEC of 21 May 1991 concerning urban waste-water  
5 treatment, EEC Council Directive.
- 6 Elías-Maxil, J.A., Van Der Hoek, J.P., Hofman, J., Rietveld, L., 2014. Energy in the urban water  
7 cycle: Actions to reduce the total expenditure of fossil fuels with emphasis on heat  
8 reclamation from urban water. *Renew. Sustain. Energy Rev.* 30, 808–820.
- 9 Eurostat, 2013. Energy, transport and environment indicators 2013. Eurostat pocketbooks.
- 10 Fikar, M., Chachuat, B., Latifi, M.A., 2005. Optimal operation of alternating activated sludge  
11 processes. *Control Eng. Pract.* 13, 853–861.
- 12 Foladori, P., Vaccari, M., Vitali, F., 2015. Energy audit in small wastewater treatment plants:  
13 methodology, energy consumption indicators, and lessons learned. *Water Sci. Technol.* 72,  
14 1007–1015.
- 15 Friedrich, E., Pillay, S., Buckley, C.A., 2009. Environmental life cycle assessments for water  
16 treatment processes—A South African case study of an urban water cycle. *Water SA* 35.
- 17 Frijns, J., Hofman, J., Nederlof, M., 2013. The potential of (waste) water as energy carrier. *Energy*  
18 *Convers. Manag.* 65, 357–363.
- 19 Funamizu, N., Iida, M., Sakakura, Y., Takakuwa, T., 2001. Reuse of heat energy in wastewater:  
20 implementation examples in Japan. *Water Sci. Technol.* 43, 277–285.
- 21 Guerrini, A., Romano, G., Indipendenza, A., 2017. Energy efficiency drivers in wastewater  
22 treatment plants: A double bootstrap DEA analysis. *Sustain. Switz.* 9.  
23 <https://doi.org/10.3390/su9071126>
- 24 Henze, M., Gujer, W., Mino, T., Van Loosdrecht, M.C.M., 2000. Activated sludge models ASM1,  
25 ASM2, ASM2d and ASM3: Scientific and technical report no. 9. IWA task group on  
26 mathematical modelling for design and operation of biological wastewater treatment. IWA  
27 Publishing, London.
- 28 Hulsbeek, J.J.W., Kruit, J., Roeleveld, P.J., Van Loosdrecht, M.C.M., 2002. A practical protocol  
29 for dynamic modelling of activated sludge systems. *Water Sci. Technol.* 45, 127–136.
- 30 Hur, D.S., 1994. A computer program for optimal aeration system design for activated sludge  
31 treatment plants (Master's Thesis). Citeseer.
- 32 IRSA, C., 1994. Metodi analitici per le acque. Ist. Poligr. E Zecca Dello Stato Roma.
- 33 Kim, Y.-H., Yoo, C., Lee, I.-B., 2008. Optimization of biological nutrient removal in a SBR using  
34 simulation-based iterative dynamic programming. *Chem. Eng. J.* 139, 11–19.
- 35 Kiselev, A., Magaril, E., Magaril, R., Panepinto, D., Ravina, M., Zanetti, M.C., 2019. Towards  
36 circular economy: Evaluation of sewage sludge biogas solutions. *Resources* 8, 91.
- 37 Kristensen, G.H., Jansen, J.L.C., Jørgensen, P.E., 1998. Batch test procedures as tools for  
38 calibration of the activated sludge model - A pilot scale demonstration. *Water Sci. Technol.*  
39 37, 235–242. [https://doi.org/10.1016/S0273-1223\(98\)00113-9](https://doi.org/10.1016/S0273-1223(98)00113-9)
- 40 Leeuw, E.J., Kramer, J.F., Bult, B.A., Wijcherson, M.H., 1996. Optimization of nutrient removal  
41 with on-line monitoring and dynamic simulation. *Water Sci. Technol.* 33, 203–209.
- 42 Liu, H., Ramnarayanan, R., Logan, B.E., 2004. Production of electricity during wastewater  
43 treatment using a single chamber microbial fuel cell. *Environ. Sci. Technol.* 38, 2281–  
44 2285.
- 45 Martin, C., Vanrolleghem, P.A., 2014. Analysing, completing, and generating influent data for  
46 WWTP modelling: a critical review. *Environ. Model. Softw.* 60, 188–201.

1 Martinello, N., 2013. Integrating experimental analyses and a dynamic model for enhancing the  
2 energy efficiency of a high-loaded activated sludge plant Master, 125.

3 Mueller, J.A., Boyle, W.C. (William C., Pöpel, H.Johannes., 2002. Aeration : principles and  
4 practice.

5 Murphy, K.L., Boyko, B.I., 1970. Longitudinal mixing in spiral flow aeration tanks. J. Sanit. Eng.  
6 Div. 96, 211–221.

7 Nelder, J.A., Mead, R., 1965. A Simplex Method for Function Minimization. Comput. J. 7, 308–  
8 313. <https://doi.org/10.1093/comjnl/7.4.308>

9 Nguyen, T.K.L., Ngo, H.H., Guo, W., Chang, S.W., Nguyen, D.D., Nghiem, L.D., Liu, Y., Ni, B.,  
10 Hai, F.I., 2019. Insight into greenhouse gases emissions from the two popular treatment  
11 technologies in municipal wastewater treatment processes. Sci. Total Environ. 671, 1302–  
12 1313.

13 Nopens, I., Benedetti, L., Jeppsson, U., Pons, M.N., Alex, J., Copp, J.B., Gernaey, K. V., Rosen,  
14 C., Steyer, J.P., Vanrolleghem, P.A., 2010. Benchmark Simulation Model No 2:  
15 Finalisation of plant layout and default control strategy. Water Sci. Technol. 62, 1967–  
16 1974. <https://doi.org/10.2166/wst.2010.044>

17 Panepinto, D., Fiore, S., Zappone, M., Genon, G., Meucci, L., 2016. Evaluation of the energy  
18 efficiency of a large wastewater treatment plant in Italy. Appl. Energy 161, 404–411.  
19 <https://doi.org/10.1016/j.apenergy.2015.10.027>

20 Reinders, M., Greditgk-Hoffmann, S., Risse, H., Lange, M., 2012. Solution approaches for energy  
21 optimization in the water sector, in: IWA World Congress on Water, Climate and Energy,  
22 Dublin, Ireland. pp. 13–18.

23 Roeleveld, P.J., Van Loosdrecht, M.C.M., 2002. Experience with guidelines for wastewater  
24 characterisation in The Netherlands, in: Water Science and Technology. pp. 77–87.  
25 <https://doi.org/10.2166/wst.2002.0095>

26 Rosso, D., Iranpour, R., Stenstrom, M.K., 2005. Fifteen Years of Offgas Transfer Efficiency  
27 Measurements on Fine-Pore Aerators: Key Role of Sludge Age and Normalized Air Flux.  
28 Water Environ. Res. 77, 266–273. <https://doi.org/10.2175/106143005x41843>

29 Ruffino, B., Campo, G., Genon, G., Lorenzi, E., Novarino, D., Scibilia, G., Zanetti, M., 2015.  
30 Improvement of anaerobic digestion of sewage sludge in a wastewater treatment plant by  
31 means of mechanical and thermal pre-treatments: Performance, energy and economical  
32 assessment. Bioresour. Technol. 175, 298–308.  
33 <https://doi.org/10.1016/j.biortech.2014.10.071>.

34 Snowling S (2016) GPS-X Technical reference. Hydromantis Environmental Software, Hamilton,  
35 Ontario.f

36 Salem, S., Berends, D., Heijnen, J.J., van Loosdrecht, M.C.M., 2002. Model-based evaluation of  
37 a new upgrading concept for N-removal. Water Sci. Technol. 45, 169–176.  
38 <https://doi.org/10.2166/wst.2002.0104>

39 Takács, I., Patry, G.G., Nolasco, D., 1991. A dynamic model of the clarification-thickening  
40 process. Water Res. 25, 1263–1271.

41 Takács, I., Vanrolleghem, P. a, 2006. Elemental Balances in Activated Sludge Modelling. IWA  
42 Publ. 1–8.

43 US EPA R R E L (1989) Design manual: fine pore aeration systems, U.S. environmental protection  
44 agency, Office of Research and Development, Center for Environmental Research  
45 Information.

1 US EPA (2012) State and local climate and energy program: water/wastewater. Available:  
2 <http://www.epa.gov/statelocalclimate/local/topics/water.html>  
3 Venkatesh, G., Brattebø, H., 2011. Energy consumption, costs and environmental impacts for  
4 urban water cycle services: Case study of Oslo (Norway). *Energy* 36, 792–800.  
5